Chapter 4

Anode Biofilm

Michal Schechter, Alex Schechter,
Shmuel Rozenfeld, Emanuel Efrat and Rivka Cahan

Additional information is available at the end of the chapter

http://dx.doi.org/10.5772/58432

1. Introduction

Microbial fuel cells (MFCs) have long been considered an attractive mean for converting various carbohydrate wastes directly into electricity using electrogenic bacterial cells in the anode compartment. Most MFCs have been operated using anaerobic or facultative aerobic bacteria which oxidize various substrates including glucose, sewage sludge and petroleum hydrocarbon [1]. Power production by MFCs varies with bacterial cell species, specific substrate concentration, cathode catalysts and the MFC configuration [2].

Typically, MFCs which were operated with a mixture of bacterial cells produced higher specific power than MFCs operated by a monoculture in the anode compartment [1]. Knowledge and understanding of the anode biofilm components, morphology formation steps and electron transfer mechanism may lead to better biofilm conductivity in MFC.

This chapter focused on biofilm definition and composition. Spectroscopic methods for anode biofilm study, including advancing real-time analysis. Power-producing bacterial cells, mechanisms of electron transfer from the biofilm to the anode and the effect of medium and pH conditions on power production.

2. Biofilm definition

The term biofilm has been proposed for a structured community of microorganisms that adheres irreversibly to surfaces (biotic or abiotic) and is enclosed in a self-developed polymeric matrix of a primarily polysaccharide material [3].

3. Biofilm composition

The biofilm matrix, which is a prerequisite for biofilm formation, consists of up to 97% water, 2-5% microbial cells, 3-6% extracellular polymeric substance (EPS) and ions [4-6]. The EPS may be hydrophilic or hydrophobic and is composed of 40-95% polysaccharides, 1-60% proteins, 1-10% nucleic acids and 1-40% lipids [7].

The EPS serves as a scaffold which holds the cell aggregates together [4]. EPS is highly hydrated, since it can incorporate large amounts of water molecules by hydrogen bonding. The microbial consortia and the environmental conditions influence the composition of the EPS [8]. The amount and thickness of the EPS increase with the biofilm's age [9].

The EPS in thin biofilms is often rich in proteins, contrary to thicker biofilms [10]. The EPS is more abundant in the interior of the biofilm, whereas cell densities are highest in the top layer [11].

As mentioned, the EPS is comprised of exopolysaccharides, proteins, nucleic acids and lipids. The exopolysaccharides in the EPS can be linear or branched, with a molecular weight of 500-2000 kDa. There are homo-polymers, e.g. cellulose, curdlan, dextran and sialic acid, but the majority are hetero-polymers composed of 2-4 types of mono-sugars such as alginate, emulsan, gellan and xanthan [6]. Nucleic acids that are found in the EPS are extracellular DNA (eDNA) that exhibit some similarities to genomic DNA but also distinct differences. In *Pseudomonas aeruginosa*, the release of eDNA is under the control of quorum sensing systems. The eDNA is necessary for the initial establishment of *P. aeruginosa* biofilms [12, 13]. Filamentous networks of eDNA were shown to stabilize the biofilm architecture. EPS lipids contribute to the hydrophobic properties of EPS [14].

The biofilm is enriched with specific protein adhesins that mediate known molecular binding mechanisms for irreversible attachment. In addition, membrane transport proteins such as porins and extracellular enzymes are up-regulated [15]. Biofilm formation occurs in a sequential process of: (i) transport of microbes to a surface by chemotaxis or Brownian motion; (ii) initial attachment; (iii) irreversible attachment of bacteria and formation of microcolonies; (iv) biofilm maturation; and (v) detachment [16].

The substratum characteristics may influence biofilm formation and morphology. Most investigators have found that microorganisms attach more rapidly to hydrophobic, nonpolar surfaces such as teflon and other plastics than to hydrophilic materials such as glass or metals [17]. Furthermore, microbial colonization increases with the increase in surface roughness [18]. The biofilm architecture changes constantly, due to external and internal processes [16]. The biofilm thickness may be affected by the number and species of microorganisms. Biofilms of pure cultures of either *Klebsiella. pneumoniae* or *P. aeruginosa* in a laboratory reactor were thinner (15 μ and 30 μ, respectively), whereas a biofilm containing both species was thicker (40 μ) [19]. Mature bacterial biofilms can adopt various architectures depending on the characteristics of the surrounding environment, such as nutrients, pH, temperature, shear forces, osmolarity and composition of the microbial consortia. The common complex biofilm is a mushroom-like structure which is surrounded by highly permeable water channels that facilitate the transport of nutrients and oxygen to the interior of the biofilm [8].

http://dx.doi.org/10.5772/58432

Cell surface-associated proteins such as pili, flagella, curli and amyloid fibers are believed to be important factors for biofilm formation [20]. Cell-to-cell signaling (quorum sensing) has been demonstrated to play a role in biofilm formation. *P. aeruginosa* produces two different quorum sensing molecules, lasR-lasI and *rhlR-rhlI,* which were shown to be involved in biofilm formation [21]. The biofilm of a double mutant produced thinner biofilms than the wild type, its cells were more densely packed, and the typical biofilm architecture was absent. Addition of the quorum sensing molecules known as homoserine lactone to a medium that contained the mutant biofilms resulted in biofilms with a structure and thickness similar to that of the wild type [17,22].

In conclusion, knowledge and understanding of the biofilm components, morphology and formation steps may lead to better biofilm conductivity in microbial fuel cells (MFC).

4. Spectroscopic methods for anode biofilm study, including advancing real-time analysis

During the last decade, most efforts in microbial fuel cell (MFC) research focused on modifications of MFC design and electrode materials, with little investigation of the properties of the anode microorganisms that are essential for maximal current production. However, understanding the functions of microbial cell surfaces requires knowledge of their chemical structural, physical properties and biological processes.

Perhaps the most challenging effort to improve MFC power production lay in the fundamental understanding of the biofilm's chemical, physical and biological characteristics. Study of the local properties of an anode biofilm is an even a greater challenge, due to the low concentration of bacterial cells. In addition to conventional methods such as scanning electron microscopy (SEM) and confocal laser scanning microscopy (CLSM), there exist modern methods such as Raman spectroscopy, Fourier transform infrared spectroscopy (FTIR) and atomic force microscopy (AFM). These latter are nondestructive methods which can probe biofilms down to single-cell surfaces with high resolution, and thereby promote better understanding of biofilm formation, functionality and activity.

In this chapter we will discuss the principle, the advantages and the disadvantages of each of the methods and the application of these techniques in MFCs.

4.1. Confocal laser scanning microscopy

Confocal laser scanning microscopy (CLSM) is often used in optical imaging of sliced microfluidic velocity fields by mapping the investigated focal plane. CLSM enables obtaining a series of optical sections of intact undisturbed biological samples as thin as 0.3 μm. Commonly used analyses that rely on staining techniques are applied to determine the architecture, spatial distribution and viability profile in microbial biofilms. The most popular application of CLSM is for identification of live and dead bacteria. Simultaneous measurements of anodic biofilms during the MFC's operation may be obscured by the need to apply labeling materials. This method is therefore used more commonly as a useful *ex situ* method [23, 24].

4.2. Scanning electron microscopy

Scanning electron microscopy (SEM) analysis provides an excellent magnification technique that uses a condensed electron beam to scan a sampled object and magnify specific regions of its surface area. Highly resolved images can be produced by SEM to provide morphological details of the surface, information on the three-dimensional topography as well as an elemental composition analysis map of the same unit area when coupled with an x-ray elemental detection sensor. SEM is therefore instrumental in a broad spectrum of scientific and industrial applications.

The main shortcomings of SEM are the relatively low resolution compared to transmission electron microscopy (TEM), which is usually higher than a few tens of nanometers and the need for a surface-conducting coating layer to avoid local charging and heating effects. Moreover, SEM is an ultra-low pressure technique. All samples must therefore withstand the low pressure inside the SEM vacuum chamber [25].

4.3. Raman spectroscopy

The Raman spectroscopy method is based on inelastic scattering of monochromatic photons, usually from a laser source. In this process, the frequency of the back-scattered photons changes their frequency due to interaction with a sample. The process begins when photons of the laser light are absorbed by the sample and are then re-emitted at a longer wavelength compared with the laser's original monochromatic frequency. This phenomenon is called the Raman frequency shift effect. This shift provides information on vibrational, rotational and other low frequency transitions at the molecular level. Raman spectroscopy is typically applied in the study of solid, liquid and gaseous samples.

The main strength of the Raman technique is its high sensitivity, the fact that it does not require any staining and its ability to generate detailed chemical and spatial information with a resolution below the diffraction limit. A combination of Raman spectroscopy with optical microscopy provides a powerful source of information which is both detailed and sensitive and can be obtained with a spatial resolution below the diffraction limit [26, 27]. The main disadvantages of the Raman technique is the weak Raman effect, which requires sensitive and highly optimized instrumentation for detection. Furthermore, fluorescence of the sample or impurities within it can mask the Raman spectrum. Sample heating through the intense laser radiation can damage the sample and distort the Raman spectrum [25].

4.4. Atomic force microscopy

Atomic force microscopy (AFM) provides one of the highest topographical profile imaging of a sampled surface, sometimes even on a nanometric scale. It does so by measuring interaction or repulsion forces between a sharp nano-size probe and a surface. The nitration distances between the tip and the sample can be as small as a few tenths of a nanometer. The AFM tip can be used either in a contact mode where the tip actually touches the surface, or in a non-contact mode where van der Waals interactions produce forces across the short distance between the tip and the surface. The forces produced by each mode of operation can be

recorded to give topographic, conductive, magnetic, mechanical (friction forces) or potential images of the surface.

In fact, AFM imaging does not require any surface modification that may damage or change the sample. Most importantly, AFM techniques are well suited to work in ambient air or in a liquid environment, including physiological conditions [25]. Therefore, the study of electrodes, biological samples, biomolecules and even living organisms can be measured rather easily by AFM. Moreover, advanced surface-imaging tools offer more than just force measurements. It can be applied to probe physical properties such as molecular interactions, surface hydrophobicity, surface charges, mechanical properties and local electrochemical properties [28]. For example, AFM enables imagining of biofilms and the EPS distribution within the biofilm [29].

The disadvantage of AFM is that the scanned area of the AFM image is rather small (few tens of microns), and it is very sensitive to externally generated electrical and mechanical noises [25].

5. Power-producing bacterial cells

Power-producing bacterial species that have exoelectrogenic activity without exogenous mediators include: *Shewanella putrefaciens, Clostridium butyricum, Desulfuromonas acetoxidans, Geobacter metallireducens, Geobacter sulfurreducens, Rhodoferax ferrireducens, Pseudomonas aeruginosa, Desulfobulbus propionicus, Geothrix fermentans, Shewanella oneidensis, Escherichia coli, Rhodopseudomonas palustris, Ochrobactrum anthropi, Desulfovibrio desulfuricans, Acidiphilium sp. Klebsiella pneumonia, Thermincola sp*. [30] and *Cupriavidus basilensis* [31]. Microorganisms which were detected on the anode of microbial electrolysis cells (MECs) include: *Stenotrophomonas, Lactobacillus, Curtobacterium, Agrobacterium, Flavobacterium, Bradyrhizobium, Pseudomonas, Desulfovibrio, Shewanella, Desulfonauticus, Xenohaliotis* and *Marinicola* [32].

Pure cultures are suitable for basic study of MFCs, since they allow analysis of electrochemical and biochemical processes as well as high reproducibility. However, mixed cultures are more suitable for industrial applications because no sterilization is required and it is not necessary to maintain anaerobic conditions via an external N_2 flow. Mixed bacteria usually produce higher power densities in MFCs than pure bacterial strains. It is important to note that the power density depends on the specific MFC configuration, electrode spacing, bacterial cell species, growth medium and the cathode catalysts [1, 2]. Thus, power densities produced in a MFC using a specific bacterium cannot be directly compared with another bacterium unless all other parameters are identical.

Exoelectrogenic bacteria transfer electrons to anodes either directly or via self-produced mediators. In the direct mechanism, electron transfer occurs via membrane-associated C-cytochrome or through conductive pili or appendages [33]. In mediated mechanisms, electron transfer between the bacterial cell and the anode surface occurs through self-produced soluble redox compounds such as flavins or pyocyanin [34]. Well-known exoelectrogens include *Geobacter* sp. and *Shewanella* sp. [35] which are known to have outer-membrane cytochromes

and conductive pili, and *Pseudomonas* sp. that produce mediators that shuttle electrons from the bacteria through the biofilm matrix to the anode [36].

6. Mechanisms of electron transfer from the biofilm to the anode

6.1. C-cytochrome

C-type cytochromes have been considered as one of the most important electron transfer strategies in current generation by exoelectrogens. C-cytochromes are heme-containing proteins which are widespread in most bacteria. *S. oneidensis* MR-1 has 42 putative C-cytochromes and 80% of them are located in the outer membrane, covering 8-34% of the cell surface. It was reported that in *Geobacter*, C-cytochromes are bound to the matrices of extracellular polymeric substrates [37]. Appendages termed bacterial nanowires that were identified in both *Shewanella* and *Geobacter* also contain surface-located C-cytochromes which are postulated to transport electrons from distant cells to electrodes [38, 39]. However, these studies are based on *in vitro* experiments and more research needs to be done to understand this mechanism [40]. *Geobacter* biofilm respiration was found to continue after the interruption of electrode polarization, since these bacteria can store electrons in the heme of the exocytoplasmic cytochromes. When the electrode was connected again, stored electrons were recovered as a current superimposed on the basal steady-state current [41].

Cytochrome genes were examined during extracellular electron transport in MEC. A total of 21 cytochrome genes were detected. Four bacterial genera contain the cytochrome genes: *Geobacter, Desulfovibrio, Rhodopseudomonas* and *Shewanella*, all of which increased over three months of the MEC reactor's performance [32]. Microarray analysis of *Geobacter sulfurreducens* thick anode biofilms (>50 μm) in MFCs revealed 13 genes in current-harvesting biofilms. Up-regulated genes included two outer C-type membrane cytochromes, OmcB and OmcZ. Down-regulated genes included the genes for the outer-membrane C-cytochromes OmcS and OmcT. Results of quantitative RT-PCR of gene transcript levels during biofilm growth were consistent with microarray results. OmcZ and the outer-surface C-type cytochrome OmcE were more abundant and OmcS was less abundant in current-harvesting cells. The role of outer-surface proteins whose genes were expressed in the current-producing biofilm versus the control biofilm which reduced fumarate were evaluated by gene deletion and its impact on current production was examined. It was found that deletion of OmcS, OmcB, or OmcE had no impact on maximum current production. Deletion of OmcZ significantly reduced power production. These results suggest that OmcZ is a key component in electron transfer in MFCs with a *G. sulfurreducens* anode [42]. In thin (ca. 10 mm) wild type biofilms, genes for OmcS and OmcE are more highly expressed than in planktonic cells grown with a soluble electron acceptor such as Fe(III) citrate [43]. CymA, which participates in many *Shewanella* anaerobic respiration processes, is a tetraheme C-cytochrome whose C-terminal is exposed to the periplasm and its N-terminal is anchored in the inner membrane. In the case of electrode reduction, a deletion of the CymA gene caused >80% decrease in current generation. CymA can interact directly with many terminal reductases in the periplasm, such as fumarate

http://dx.doi.org/10.5772/58432

reductase and nitrate reductase. Bacterial two-hybrid showed pair-wise interactions among CymA, MtrA and some other periplasmic redox proteins, indicating that CymA is the major electron conduit to the periplasmic space and can interact directly with periplasmic redox proteins by forming a transient protein complex [44].

Okamoto et al identified voltammetry signals of outer membrane C-cytochrome in monolayer biofilms of *S. oneidensis* [45]. Okamoto et al analyzed monolayer and multilayer biofilms of *S. oneidensis* on tin-doped indium oxide electrodes and compared the respective amounts of electroactive C-cytochrome using voltammetry techniques. The scan-rate dependence of cyclic voltammograms was used to investigate the role of C-cytochrome in the transfer of respiratory electrons to distant tin-doped indium oxide electrodes. Electron conduction in *S. oneidensis* MR-1 multilayer biofilms was demonstrated to be mediated by sequential redox cycling of outer membrane C-cytochrome under normal physiological conditions. It was also demonstrated that the electron transport outer membrane C-cytochrome conduit across the biofilms contributed to the anodic current generation [40].

Immunogold labeling of the outer-surface C-type cytochrome OmcZ showed that when *G. sulfurreducens* grew as a biofilm on a graphite electrode that served as an anode and sole electron acceptor for growth, OmcZ was highly concentrated at the biofilm–electrode interface. Control biofilms which were grown on the same graphite material but with fumarate as the electron acceptor did not have OmcZ accumulations at the biofilm–electrode interface. The researchers suggested that OmcZ may serve as an electrochemical gate facilitating electron transfer from *G. sulfurreducens* biofilms to the anode surface [46]. Direct current surface-enhanced infrared (IR) absorption spectroscopy and FTIR demonstrated a linear correlation between the increasing presence of *Geobacter sulfurreduces* protein and current production. This result may confirm that the extracellular cytochromes [47] are responsible for the electron transfer to the gold electrode [48].

Eaktasang et al. electrochemically oxidized the surface of a graphite felt electrode with a strong acid in order to stimulate current production in the MFC. FT-IR was used to examine the chemical property changes in the graphite felt surfaces which were induced by its electrochemical oxidation using acid treatment. Current production in the MFC equipped with the surface-modified graphite anode was about 40% higher than that obtained from the MFC of a bare graphite anode. FT-IR spectra of surface-modified felt and bare graphite felt showed a notable broad band at 3264 cm^{-1} ascribed to stretching vibration of OH within –COOH, a broad peak at 1560cm^{-1} ascribed to C=O of ketone and carboxyl groups, and a peak at 1419 cm^{-1} ascribed to bending vibration of –OH. The relative intensities of the abovementioned peaks increased significantly after electrochemical oxidation treatment of graphite felt, indicating that alcohol and carboxyl functional groups formed on the surface of the graphite-felt hydrogen bonding with peptide bonds in the bacterial cytochrome. They also demonstrated that the carboxylic acid terminus of gold-modified electrodes can facilitate the binding with cytochrome on its surface, and as a result, current production increased due to the enhanced transfer of electrons from the interior of the cell [49]. *In vitro* and *in vivo* experiments led to the proposal of several models based on the redox properties of bacterial C-cytochromes. A 4-step mechanism for electron transfer in *Geobacter* biofilms was proposed: step 1, acetate uptake and electron

transfer to periplasmic cytochromes; step 2, subsequent electron transfer to the exocytoplasmic cytochromes; step 3, electron transport along the biofilm matrix cytochromes; and step 4, transfer between the interfacial cytochromes and the electrode [41].

6.2. Pili

Genes encoding proteins with a PilZ domain were deleted from the G. sulfurreducens genome in an attempt to study the importance of pili to biofilm conductivity. The mutant strain designated as strain CL-1 produced more pili than the wild type strain and formed 6-fold more conductive biofilms than the wild type strain. Heme-staining revealed a higher abundance of cytochrome with a molecular weight consistent with OmcS in CL-1 and Western blot analysis with OmcS-specific antiserum confirmed higher production of OmcS in CL-1. Immunogold labeling coupled with TEM demonstrated that OmcS was localized on the pili of CL-1 [50]. Multilayer biofilms of *Geobacter sulfurreducens* on the anode surface of a MFC remained viable even at a distance from the anode. There was no decrease in the efficiency of current production with an increase in the thickness of the biofilm. Genetic studies demonstrated that efficient electron transfer through the biofilm required the presence of electrically conductive pili which represent an electronic network promoting long-range electrical transfer in an energy-efficient manner in the MFC [38].

G. sulfurreducens KN400 bacterial cells which were selected after 5 months of incubation at-400 mV produced higher current and power densities than the original inoculum (strain DL1). The enhanced capacity for current production in KN400 was associated with a greater abundance of electrically conductive microbial nanowires than DL1 and lower internal resistance in KN400 fuel cells. KN400 produced flagella, whereas DL1 does not. The changes in outer surface components were associated with a greater propensity of strain KN400 to stick to surfaces than strain DL1. KN400 cells grown with fumarate as the electron acceptor were clumpy and strongly adhered to the glass surface of the culture tubes. This research showed that microorganisms' ability to electrochemically interact with electrodes can be enhanced with the appropriate selective pressure and that improved current production is associated with clear differences in the properties of the outer surface of the cell that may provide better microbe–electrode interactions [51].

The AFM technique, together with electrochemical measurements by scanning tunneling microscopy (STM), allowed mapping of conducting substrates and microbial pili in MFCs studies. These two techniques enabled identification of the pili on *Geobacter* species. The existence of such pili raises the possibility of long-range direct electron transfer from each microbe to the electrode [36, 48]. El-Naggar et al. evaluated transport along the bacterial nanowires by conducting probe AFM at several points alongside a single nanowire using a metallic electrode and a conductive AFM tip. *S. oneidensis* MR-1 nanowires were electrically conductive along micrometer-length scales, yielding a corresponding electron transport rate, at 100 mV, of about 109 electrons per second, with an estimated resistance of 1 Ω (Fig 1). It was also found that mutants deficient in genes for the C-type decaheme-cytochromes MtrC and OmcA produced supplements that are morphologically consistent with bacterial nanowires, but were found to be nonconductive [52].

http://dx.doi.org/10.5772/58432

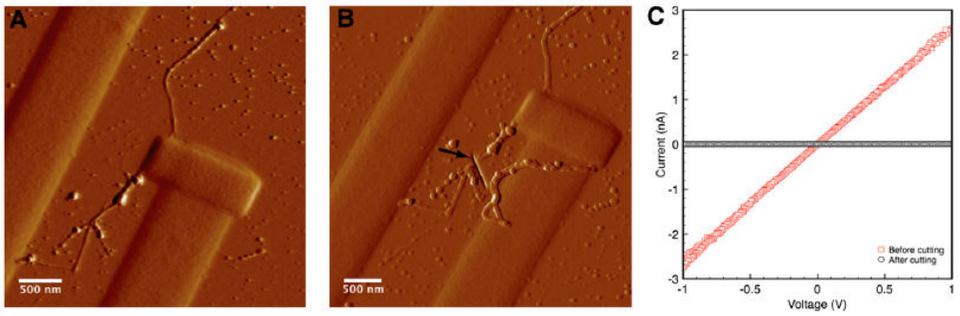

Figure 1. Measuring electrical transport along a bacterial nanowire. (A) Tapping-mode atomic force microscopy (AFM) amplitude image detailing the contact area with the bacterial nanowire from Fig. 1. (B) Contact-mode AFM deflection image of the junction after cutting the nanowire with FIB milling. The arrow marks the cut location. (C) Current-voltage curve of the bacterial nanowire (ramp-up and ramp-down) both before (red) and after (black) cutting the nanowire [52].

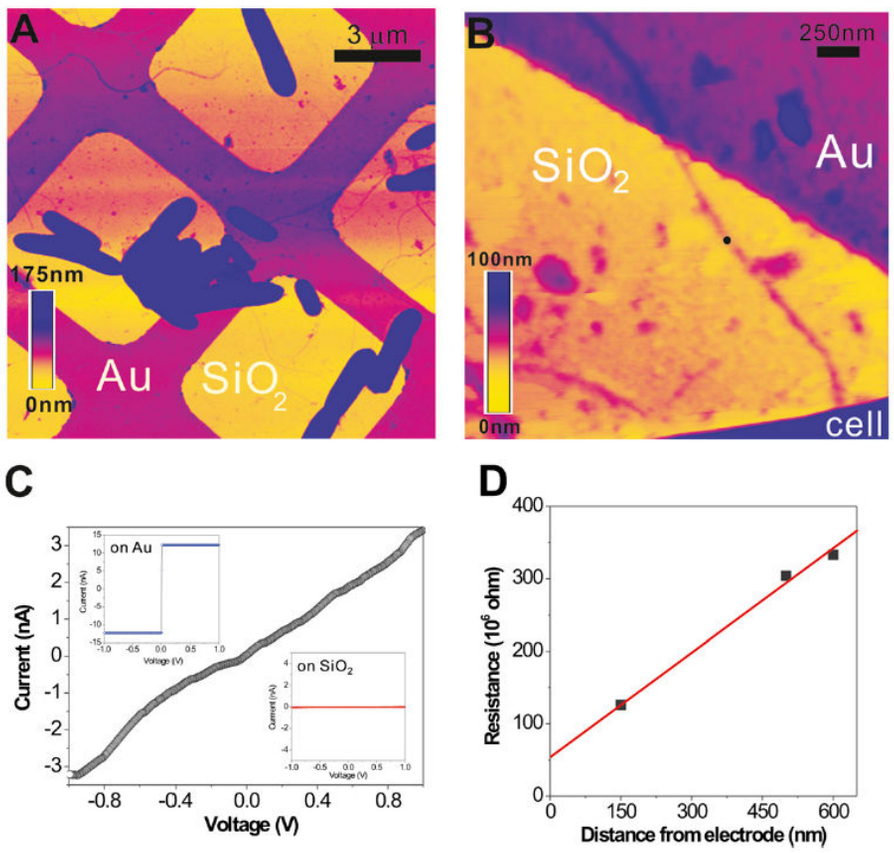

Figure 2. CP-AFM of a bacterial nanowire. (A) Topographic AFM image showing air-dried S. oneidensis MR-1 cells and extracellular appendages deposited randomly on a SiO2/Si substrate patterned with Au microgrids. (B) Contact mode AFM image showing a nanowire reaching out from a bacterial cell to the Au electrode. (C) An I-V curve obtained by probing the nanowire at a length of 600 nm away from the Au electrode (at the position marked by the black dot in B). (Inset) The I-V curves obtained on bare Au and SiO2, respectively. (D) A plot of total resistance as a function of distance between AFM tip and Au electrode [52].

7. The effect of medium and pH conditions on power production

The effects of anodic pH on electricity production in two-chamber MFCs inoculated with anaerobic activated sludge were examined. The maximum power density was 1170±58 mWm^2 with a current density of 0.18 $mA \times cm^{-2}$ at pH 9.0, which was 29% and 89% higher than in MFCs operated at pH 7.0 and 5.0, respectively. Electrochemical measurements demonstrated that the environmental pH may influence the electron transfer kinetics of the anodic biofilms. At pH 9.0, the apparent electron transfer rate constant and exchange current density were greater, whereas charge transfer resistance was smaller than under other pH conditions. SEM analysis reveled better biofilm formation at pH 9.0 compared to pH 7.0 and 5.0. The biofilm at pH 9.0 showed increased electron transfer efficiency with respect to the electrocatalytic current, electron transfer rate, exchange current density, and charge transfer resistances, compared with biofilms at pH 7.0 and 5.0. These results demonstrate that electrochemical interactions between bacteria and electrodes in MFCs are greatly enhanced under alkaline conditions, which can an important reason for the improved current production in MFCs [53]. It should be noted that the cathodic potentials were almost identical under all pH conditions, whereas the anodic potentials varied. The anode that operated at pH 9.0 had the most negative individual potentials in the entire current range, whereas the anode at pH 5.0 had the most positive individual potentials. The variations in the power outputs thus resulted from the anodes under different pH conditions [53].

The performance of two dual-chambered mediators-less MFCs was evaluated at different sludge loading rates and pH environments. A maximum volumetric power of 15.51 W/m^3 and 36.72 W/m^3 was obtained in MFC-1 (feed pH 6.0) and MFC-2 (feed pH 8.0), respectively. These results indicate that higher feed pH (8.0) led to higher power production [54]. Zhuang et al. discovered that an alkaline anode (pH 10) led to higher power production during wastewater treatment compared to a MFC which worked at neutral pH. Their assumption is that there methanogenesis is suppressed at higher pHs, and this contributes to a significant enhancement of coulombic efficiency [55]. In contradistinction to the abovementioned studies, there are several studies which described that higher power production was obtained in natural or acidic environments. An air-cathode MFC which operated with a mixed bacterial culture at different pHs showed that the anodic microbial process preferred a neutral pH and that microbial activities decreased at higher or lower pHs [56]. A MFC with a pure culture of *Enterobacter cloacae* was evaluated as a function of variations in the pH microenvironment. Operation under pH 6.5 and 7.4 led to maximum current generation of 0.40 mA and 0.42 mA, respectively. However, MFC operation under higher pH environments of 8.5 and 9.5 led to a maximum current generation of only 0.38 mA and 0.27 mA, respectively [57].

In conclusion, we assume that MFC power production is dependent on the pH environment and may correlate with the bacterial cell anode species.

http://dx.doi.org/10.5772/58432

8. Anode biofilm thickness, morphology, viability and conductivity

CSLM analyses revealed a correlation between current and increasing coverage of the anode surface with cells. The average height of the biofilm pillars at currents nearing the maximum current outputs in batch mode was 40 μm (±6 μm), and some cell clusters were as high as 50 μm. Protein measurements of the biofilm biomass at different points during current production indicated a direct linear increase in the amount of biomass on the anodes as the current increased and the biofilms developed. Viability staining indicated that during biofilm development, cells at a distance from the electrode surface remained viable, metabolically active and involved in electron transfer to the anode [38].

Geobacter can form multi-microbe thick, more than 20-cell length, persistent biofilms when the anode serves as their terminal electron acceptor. This phenomenon was not observed in the presence of insoluble oxidants for respiration. The combination of robust direct electron transfer and high cell surface density enables *Geobacter* biofilms to achieve higher anodic current densities than any other species [58].

Three MFCs (plain graphite electrodes, air cathode, Nafion membrane) were operated separately with variable biofilm coverage [control; anode surface coverage (0%), partially developed biofilm (coverage ~44%) and fully developed biofilm (coverage of ~96%)] under acidophilic conditions (pH 6) at room temperature. Higher specific power production [29 mW/kg CODR (CW and DSW)], specific energy yield [100.46 J/kg VSS (CW)], specific power yield [0.245 W/kg VSS (DSW); 0.282 W/kg VSS (CW)] and substrate removal efficiency of 66.07% (substrate degradation rate, 0.903 kg COD/m^3-day) were observed, especially with fully developed biofilm operation [59].

The behavior of MFCs during initial biofilm growth and characterization of anodic biofilm were studied using two-chamber MFCs with activated sludge as inoculum. When the biofilms were well developed, a maximum closed circuit potential of 0.41 V and 0.37 V (1000 Ω resistor) was achieved using acetate and glucose, respectively. SEM analysis revealed rod-shaped cells, 0.2-0.3 mm wide by 1.5-2.5 mm long, in the anode biofilm in the acetate-fed MFC, mainly arranged in a monolayer. The biofilm in the glucose-fed MFC was made of cocci-shaped cells in chains and a thick matrix [60. A MFC was operated with a pure culture of *Cupriavidus basilensis* bacterial cells grown in a defined medium containing acetate or phenol. Operating this mediator-less MFC under a constant external resistor of 1 kΩ with acetate or phenol led to a current generation of 902 and 310 mA m^{-2}, respectively. SEM and confocal microscopy analyses demonstrated a developed biofilm with pili/appendages and a live anode *C. basilensis* population which was stained with a LIVE/DEAD viability kit and further analyzed by CSLM (Fig 3) [31].

Electron transfer between bacterial cells and the electrode is one of the major blockages to a desired power density. A direct electron transfer process between *P. aeruginosa* bacterial cells and the electrode was investigated using cationic reagents which are known to "perforate" the bacterial membrane. Three reagents, chitosan, ethylenediaminetetraacetic acid (EDTA) and polyethyleneimine (PEI), were explored. The surface morphologies of chemically treated

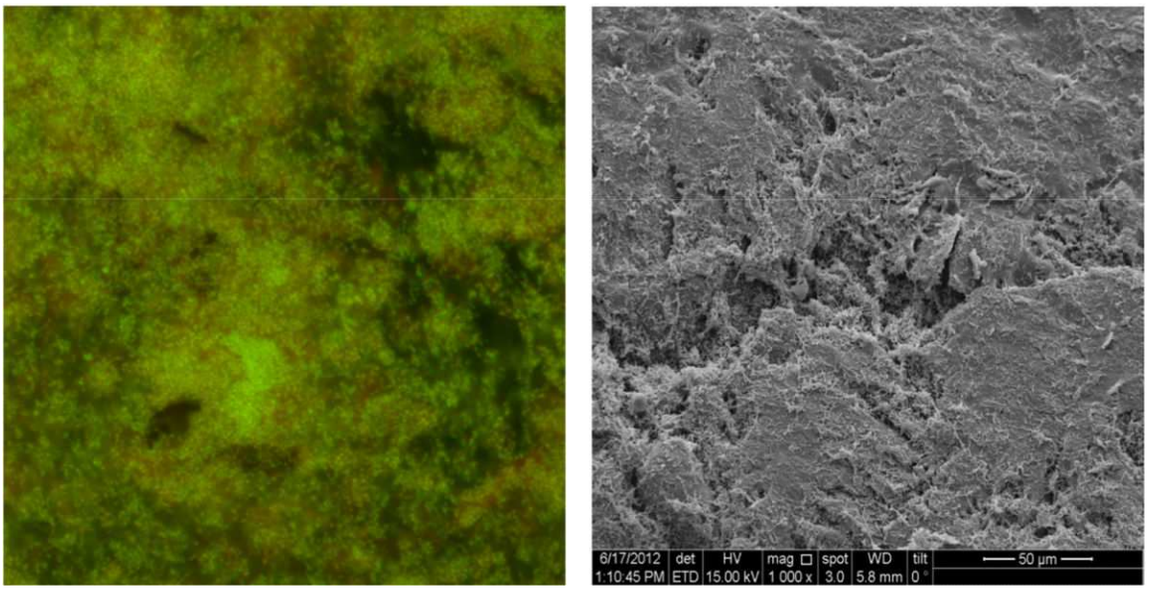

Figure 3. *Cupriavidus basilensis* biofilm grown on a graphite anode in MFC. CSLM micrograph, magnification of 40 (A). SEM micrograph, magnification of 1,000 (B).

P. aeruginosa cells were examined with SEM and AFM images. The results showed that the chemical treatment caused changes in the cell shape and perforated bacterial cells, contrary to the original *P. aeruginosa* cells that were plump and smooth. The cells were flattened with pores and clusters on the surface. The chemical treatment disorganized the outer membrane of *P. aeruginosa* which resulted in higher permeability, like "drilling", which significantly improved electron transfer for high power density MFCs. Cyclic voltammograms (CV) of the anaerobically activated control and perforated *P. aeruginosa* cells were measured in glucose-free medium and showed two pairs of redox peaks at-0.59 and-0.47 V. The two redox waves represented different electron transfer mechanisms of this bio-anode. The output current profiles at a constant load of chitosan, EDTA-and PEI-treated cells were much higher than in control cells, and the PEI-treated cell catalysts produced the highest discharge (oxidation) current density, which parallels the result of the CV experiment. The polarization curves revealed that the PEI-treated cell has much lower polarization for better energy conversion efficiency than the control cells. It was explained that the increased permeability of the bacterial outer membrane by the large pores and channels facilitates the transport of redox mediators and catabolic enzymes through the cell membrane and thus provides faster electron transfer [61].

Introducing a pH-sensitive fluoroprobe into the anode chamber revealed a strong pH gradient within the *G. sulfurreducens* anode biofilm. The pH decreased with increased proximity to the anode surface and from the exterior to the interior of the biofilm pillars. pH levels near the anode surface were as low as 6.1 compared to pH 7 near the cathode. Various controls demonstrated that proton accumulation was associated with current production. Decreasing the pH of the culture medium from 7 to 6 limited the growth of *G. sulfurreducens*. The results demonstrated that it is feasible to non-destructively monitor the activity of anode biofilms in

http://dx.doi.org/10.5772/58432

real time. It was also suggested that the accumulation of protons that are released from organic matter oxidation within anode biofilms can limit current production [62].

Millo et al. employed surface-enhanced resonance Raman (SERR) spectroscopy in combination with CV analysis. This technique, performed under strict electrochemical control, reveals the redox, coordination and spin states of the heme iron in addition to the nature of its axial ligand. Furthermore, by applying *in situ* SERR spectroscopy electrochemical analysis on a catalytically active biofilm grown on silver electrodes, it was revealed that two bis (histidine) coordinated heme cytochrome redox couples are involved in the mediated electron transfer between the bacteria and the electrode [63].

Liu et al. showed that graphene modification improved power density and energy conversion efficiency by almost 3 times that of a *P. aeruginosa* mediator-less MFC. Raman analysis revealed that the improvement was credited to the high biocompatibility of graphene which promotes bacterial growth on the electrode surface and results in the creation of more direct electron transfer activation centers and stimulates excretion of mediating molecules for higher electron transfer [65]. Raman spectroscopy analysis at different growth stages revealed changes in the vibrational properties of *Geobacter* Cyt *c* resulting from shifts in the anodic potential between different redox conditions [65].

In conclusion, the biofilm strain composition, components, morphology and thickness play a major role in the electrochemical process in MFCs, and show marked influence on bioelectricity production. Changes in biofilm parameters may influence the anode electrochemical characteristics and performance in a MFC. It is therefore important to understand the characteristics, structure and composition of the biofilm in order to ensure optimized operation of MFCs.

Acknowledgements

This chapter was supported in part by the Research Authority of Ariel University, the Israel Ministry of Environmental Protection and the Samaria and Jordan Rift Valley Regional R&D Center.

Author details

Michal Schechter[1], Alex Schechter[2], Shmuel Rozenfeld[1], Emanuel Efrat[1] and Rivka Cahan[1*]

*Address all correspondence to: rivkac@ariel.ac.il

1 Department of Chemical Engineering, Ariel University, Ariel, Israel

2 Department of Biological Chemistry, Ariel University, Ariel, Israel

References

[1] Rabaey K., Boon N., Hofte M., Verstraete W. Microbial Phenazine Production Enhances Electron Transfer in Biofuel Cells. Environmental Science and Technology 2005; 39(9) 3401–3408.

[2] Liu BF., Ren NQ., Tang J., Ding J., Liu WZ., Xu JF., Cao GL., Guo WQ., Xie G.J. Bio-Hydrogen Production by Mixed Culture of Photo-and Dark-Fermentation Bacteria. International Journal of Hydrogen Energy 2010; 35(19) 2858–2862.

[3] Donlan RM., Biofilms: Microbial Life on Surfaces. Emerging Infectious Diseases Journal 2002; 8(9) 881-890.

[4] Branda SS., Vik S., Friedman L., Kolter R. Biofilms: the Matrix Revisited. Trends Microbiology. 2005; 13(1) 20-26.

[5] Flemming HC., Neu TR., Wozniak DJ. The EPS Matrix: The House of Biofilm Cells. Journal of Bacteriology. 2007; 189(22) 7945-7947.

[6] Sutherland IW. The Biofilm Matrix-an Immobilized but Dynamic Microbial Environment. Trends Microbiology. 2001; 9(5) 222-227.

[7] Flemming HC., Wingender J., Extracellular Polymeric Substances (EPS): Structural, Ecological and Technical aspects, in Encyclopedia of environmental microbiology, Bitton G, Editor. John Wiley & Sons: New York. 2002; p. 1223-1231.

[8] Kolter R., Greenberg EP. Microbial Sciences: the Superficial Life of Microbes. Nature. 2006; 441(7091) 300-302.

[9] Leriche V., Sibille P., Carpentier B. Use of an Enzyme-Linked Lectinsorbent Assay to Monitor the Shift in Polysaccharide Composition in Bacterial Biofilms. Applied and Environmental Microbiology 2000; 66(5) 1851–1856.

[10] [10] Celmer D., Oleszkiewicz JA, Cicek N. Impact of Shear Force on the Biofilm Structure and Performance of a Membrane Biofilm Reactor for tertiary Hydrogen-Driven Denitrification of Municipal Wastewater. Water Research. 2008; 42(12) 3057-3065.

[11] Gieseke A., Arnz P., Amann R., Schramm A. Simultaneous P and N Removal in a Sequencing Batch Biofilm Reactor: Insights from Reactor-and Microscale Investigations. Water Research. 2002; 36(2) 501-509.

[12] Allesen-Holm M., Barken KB., Yang L., Klausen M., Webb JS., Kjelleberg S., Molin S., Givskov M., Tolker-Nielsen T. A Characterization of DNA Release in *Pseudomonas aeruginosa* Cultures and Biofilms. Molecular Microbiology. 2006; 59(4) 1114–1128.

[13] Whitchurch CB., Tolker-Nielsen T., Ragas PC., Mattick JS. Extracellular DNA Required for Bacterial Biofilm Formation. Science. 2002; 295 1487.

[14] Conrad A., KontroM., Keinänen MM., Cadoret A., Faure P., Mansuy-Huault L., Block JC. Fatty Acids of Lipid Fractions in Extracellular Polymeric Substances of Activated Sludge Flocs. Lipids. 2003; 38(10)1093-1105.

[15] Dunne WM. Bacterial Adhesion: Seen Any Good Biofilms Lately? Clinical Microbiology Reviews. 2002; 15(2) 155-166.

[16] Tolker-Nielsen T., Brinch UC., Ragas PC., Andersen JB., Jacobsen CS., Molin S. Development and Dynamics of *Pseudomonas* sp. Biofilms. Journal of Bacteriology. 2000; 182(22) 6482–6489.

[17] Fletcher M., Loeb GI. Influence of Substratum Characteristics on the Attachment of a Marine *Pseudomonad* to Solid Surfaces. Applied and Environmental Microbiology. 1979; 37(1) 67–72.

[18] Characklis WG., McFeters GA., Marshall KC. Physiological Ecology in Biofilm Systems. In: Characklis WG, Marshall KC, editors. Biofilms. New York: John Wiley & Sons; 1990. p. 341–94.

[19] James GA., Beaudette L., Costerton JW. Interspecies Bacterial Interactions in Biofilms. Journal of Industrial Microbiology. 1995;15(4) 257-62.

[20] Gohl O., Friedrich A., Hoppert M., Averhoff B. The Thin Pili of *Acinetobacter* sp. Strain BD413 Mediate Adhesion to Biotic and Abiotic Surfaces. Applied and Environmental Microbiology. 2006; 72(2) 1394-1401.

[21] Davies DG., Parsek MR., Pearson JP., Iglewski BH., Costerton JW., Greenberg EP. The Involvement of Cell-to-Cell Signals in the Development of a Bacterial Biofilm. Science. 1998; 280(5361) 295–298.

[22] Xie H., Cook GS., Costerton JW., Bruce G., Rose TM., Lamont RJ. Intergeneric Communication in Dental Plaque Biofilms. Journal of Bacteriology. 2000; 182 7067–7069.

[23] Astner S., Ulrich M. Confocal Laser Scanning Microscopy. Hautarzt. 2010; 61 421-428.

[24] Murphy DB., Davidson MW. Confocal Laser Scanning Microscopy. In: Fundamentals of Light Microscopy and Electronic Imaging. 2012; 265-305.

[25] Niemantsverdriet JW. Spectroscopy in catalysis: WILEY-VCH Verlag GmbH & Co. kgAa.2007.

[26] Neugebauer U., Rösch P., Schmitt M., Popp J., Julien C., Rasmussen A., Budich C., Deckert V. On the Way to Nanometer-Sized Information of the Bacterial Surface by Tip-Enhanced Raman Spectroscopy. ChemPhysChem. 2006; 7(7) 1428-1430.

[27] Pradhan N., Pradhan SK., Nayak BB., Mukherjee PS., Sukla LB., Mishra BK. Micro-Raman analysis and AFM imaging of *Acidithiobacillus ferrooxidans* biofilm grown on uranium. Research in Microbiology. 2008; 159(7-8) 557-561.

[28] Dufrêne YF. Atomic Force Microscopy of Fungal Cell Walls: an Update. Yeast 2010; 27(8) 465-471.

[29] Beech IB., Smith JR., Steele AA., Penegar I., Campbell SA. The Use of Atomic Force Microscopy for Studying Interactions of Bacterial Biofilms with Surfaces. Colloids and Surfaces B: Biointerfaces. 2002; 23 231-247.

[30] Logan BE. Exoelectrogenic Bacteria that Power Mmicrobial Fuel Cells. Nature Reviews. 2009; 7 375-381.

[31] Friman H., Schechter A., Ioffe Y., Nitzan Y., Cahan R. Current Production in a Microbial Fuel Cell Using a Pure Culture of *Cupriavidus basilensis* Growing in Acetate or Phenol as a Carbon Source. Microbial Biotechnology. 2013; 6(4) 425-34.

[32] Liu W., Wang A., Sun D., Ren N., Zhang Y., Zhou J. Characterization of Microbial Communities During Anode Biofilm Reformation in a Two-Chambered Microbial Electrolysis Cell (MEC). Journal of Biotechnology. 2012; 157(4) 628–632.

[33] Mehta T., Coppi MV., Childers SE., Lovley DR. Outer Membrane C-Type Cytochromes Required for Fe(III) and Mn(IV) Oxide Reduction in *Geobacter sulfurreducens*. Applied and Environmental Microbiology 2005; 71(12) 8634-8641.

[34] Enrico M., Baron DB., Shikhare ID., Coursolle D., Gralnick JA., Bond DR. *Shewanella* Secretes Flavins that Mediate Extracellular Electron Transfer. Proceedings of the National Academy of Sciences. 2008;105(10) 3968-3973.

[35] Kim JR., Jung SH., Regan JM., Logan BE. Electricity Generation and Microbial Community Analysis of Alcohol Powered Microbial Fuel Cells. Bioresource Technology. 2007; 98 2568–2577.

[36] Reguera G., McCarthy KD., Mehta T., Nicoll JS., Tuominen MT., Lovley DR.. Extracellular Electron Transfer via Microbial Nanowires. Nature 2005; 435(7045) 1098–1101.

[37] Richter H., Nevin KP., Jia H., Lowy DA., Lovley DR. Tender LM. Cyclic Voltammetry of Biofilms of Wild Type and Mutant *Geobacter sulfurreducens* on Fuel Cell Anodes Indicates Possible Roles of OmcB, OmcZ, Type IV Pili, and Protons in Extracellular Electron Transfer. Energy and Environmental Science. 2009; 2 506–516.

[38] Reguera G., Nevin KP., Nicoll JS., Covalla SF., Woodard TL., Lovley DR. Biofilm and Nanowire Production Leads to Increased Current in *Geobacter sulfurreducens* Fuel Cells. Applied and Environmental Microbiology. 2006; 72(11) 7345–7348.

[39] Gorby YA., Yanina S., McLean JS., Rosso KM., Moyles D., Dohnalkova A., Beveridge TJ., Chang IS., Kim BH., Kim KS., Culley DE., Reed SB., Romine MF.,Saffarini DA., Hill EA., Shi L., Elias DA., Kennedy DW., Pinchuk G., Watanabe K., Ishii S., Logan B., Nealson KH., Fredrickson JK. Electrically Conductive Bacterial Nanowires Produced by *Shewanella oneidensis* Strain MR-1 and Other Microorganisms, Proceedings of the National Academy of Sciences. 2006; 103 (30) 11358–11363.

[40] Okamoto A., Hashimoto K., Nakamura R. Long-range Electron Conduction of *Shewanella* Biofilms Mediated by Outer Membrane C-type Cytochromes. Bioelectrochemistry 2012; 85 61-65.

[41] Bonanni PS., Schrott GD., Robuschi L., Busalmen JP. Charge Accumulation and Electron Transfer Kinetics in *Geobacter sulfurreducens* Biofilms Energy and Environmental Science. 2012; 5 6188–6195.

[42] Nevin KP., Kim BC., Glaven RH., Johnson JP., Woodard TL., Methe BA., DiDonato RJ., Covalla SF., Franks AE., Liu A., Lovley DR. Anode Biofilm Transcriptomics Reveals Outer Surface Components Essential for High Density Current Production in *Geobacter sulfurreducens* Fuel Cells. PLoS ONE 2009; 4(5) 1-10.

[43] Holmes DE., Chaudhuri SK., Nevin KP., Mehta T., Methe BA., Liu A., Ward JE., Woodard TL., Webster J. Lovley DR. Environmental Microbiology. 2006; 8(10) 1805–1815.

[44] Yanga Y., Xua M., Guoa J., Sun G. Bacterial extracellular electron transfer in bioelectrochemical systems. Process Biochemistry. 2012; 47 1707–1714

[45] Okamoto A., Nakamura R., Ishii K., Hashimoto K. In vivo Electrochemistry of C Type Cytochrome-Mediated Electron-Transfer with Chemical Marking. Chem BioChem 2009; 10 2329–2332.

[46] Inoue K., Leang C., Franks AE., Woodard TL., Nevin KP. Lovley DR. Specific Localization of the *c*-Type Cytochrome OmcZ at the Anode Surface in Current-Producing Biofilms of *Geobacter sulfurreducens*. Environmental Microbiology Reports.2011; 3 211–217.

[47] Busalmen JP., Esteve-Nunez A., Berna A., Feliu JM. C-type Cytochromes Wire Electricity-Producing Bacteria to Electrodes. Angewandte Chemie International Edition. 2008; 47 (26) 4874-4877.

[48] Zhao F., Slade RC., Varcoe JR. Techniques for the Study and Development of Microbial Fuel Cells: an Electrochemical Perspective. Chemical Society Review. 2009; 38(7) 1926-1939.

[49] Eaktasang N., Kim D., Lee JW., Park KY., and Kim HS. Enhancement of Electron Transfer by Electrochemical Treatment of Electrode in the Microbial Fuel Cell. In: International Conference on Chemical, Environmental Science and Engineering Pattaya (Thailand).2012; p44-46.

[50] Leang C., Malvankar NS., Franks AE., Nevin KP. Lovley DR. Engineering *Geobacter sulfurreducens* to Produce a Highly Cohesive Conductive Matrix with Enhanced Capacity for Current Production. Energy and Environmental Science. 2013; 6 1901–1908.

[51] Yi H., Nevin KP., Kim B-C., Franks AE., Klimes A., Tender LM., Lovley DR. Selection of a Variant of *Geobacter sulfurreducens* with Enhanced Capacity for Current Production in Microbial Fuel Cells. Biosensors and Bioelectronics. 2009; 24(12) 3498-3503.

[52] El-Naggar MY., Wanger G., Leung KM., Yuzvinsky TD., Southam G., Yang J., Lau WM, Nealson KH., Gorby YA. Electrical Transport Along Bacterial Nanowires from *Shewanella oneidensis* MR-1. Proceedings of the National Academy of Sciences. 2010; 107(42) 18127-18131.

[53] Yuan Y., Zhao B., Zhou S., Zhong S., Zhuang L. Electrocatalytic Activity of Anodic Biofilm Responses to pH Changes in Microbial Fuel Cells. Bioresource Technology 2011; 102 (13) 6887–6891.

[54] Behera MM., Ghangrekar MM.. Performance of Microbial Fuel Cells in Response to Change in Sludge Loading Rate at Different Anodic Feed pH. Bioresource Technology 2009; 100(21) 5114–5121.

[55] Zhuang L., Zhou SG., Li YT., Yuan Y.. Enhanced Performance of Air-Cathode Two-Chamber Microbial Fuel Cells with High-pH Anode and Low-pH Cathode. Bioresource Technology. 2010; 101(10) 3514–3519.

[56] He Z., Huang YL., Manohar AK., Mansfeld F. Effect of Electrolyte pH on the Rate of the Anodic and Cathodic Reactions in an Air-Cathode Microbial Fuel Cell. Bioelectrochemistry 2008; 24 78–82.

[57] Nimje VR., Chen CY., Chen CC., Tsai JY., Chen HR., Huang YM., Jean JS., Chang YF., Shih RC. Microbial Fuel Cell of *Enterobacter cloacae*: Effect of Anodic pH Microenvironment on Current, Power Density, Internal Resistance and Electrochemical Losses. International Journal of Hydrogen Energy. 2011; 36 11093-11101.

[58] Bond DR., Strycharz-Glaven SM., Tender LM., Torres CI. On Electron Transport Tthrough Geobacter Biofilms. ChemSusChem, 2012; 5(6) 1–8.

[59] Mohan SV., Raghavulu SV., Sarma PN. Influence of Anodic Biofilm Growth on Bioelectricity Production in Single Chambered Mediator Less Microbial Fuel Cell Using Mixed Anaerobic Consortia. Biosensors and Bioelectronics 2008; 24(1) 41–47.

[60] Yang S., Du F., Liu H. Characterization of Mixed-Culture Biofilms Established in Microbial Fuel Cells. Biomass and Bioenergy 2012; 46 531-537.

[61] Liu J., Qiao Y., Lu ZS., Song H., Li CM. Enhance Electron Transfer and Performance of Microbial Fuel Cells by Perforating the Cell Membrane. Electrochemistry Communications. 2012; 15(1) 50-53.

[62] Franks AE., Nevin KP., Jia H., Izallalen M., Woodard TL., Lovley DR. Novel Strategy for Three-Dimensional Real-Time Imaging of Microbial Fuel Cell Communities: Monitoring the Inhibitory Effects of Proton Accumulation Within the Anode Biofilm. Energy & Environmental Science. 2009; 2 113-119.

[63] Millo D., Harnisch F., Patil SA., Ly HK., Schröder U., Hildebrandt P. In Situ Spectroelectrochemical Investigation of Electrocatalytic Microbial Biofilms by Surface-Enhanced Resonance Raman Spectroscopy. Angewandte Chemie International Edition. 2011; 50(11) 2625-2627.

[64] Liu J, Qiao Y, Guo CX, Lim S, Song H, Li CM. Graphene/Carbon Cloth Anode for High-Performance Mediatorless Microbial Fuel Cells. Bioresource Technology. 2012; 114 275-280.

[65] Virdis B., Harnisch F., Batstone DJ., Rabaey K., Donose BC. Non-Invasive Characterization of Electrochemically Active Microbial Biofilms Using Confocal Raman Microscopy. Energy and Environmental Science. 2012; 5(5) 7017-7024.

IntechOpen

IntechOpen